Synthesis of Low-Sidelobe Stepped-Amplitude Aperiodic Phased Arrays

Aslan, Yanki ; Roederer, Antoine; Yarovoy, Alexander

DOI
10.23919/EuCAP51087.2021.9411337

Publication date
2021

Document Version
Final published version

Published in
2021 15th European Conference on Antennas and Propagation (EuCAP)

Synthesis of Low-Sidelobe Stepped-Amplitude Aperiodic Phased Arrays

Yanki Aslan[1], Antoine Roederer[2], Alexander Yarovoy[3]
Microwave Sensing, Signals and Systems Group, Department of Microelectronics,
Faculty of Electrical Engineering, Mathematics, and Computer Science,
Delft University of Technology, Delft, The Netherlands
{[1]Y.Aslan, [2]A.G.Roederer, [3]A.Yarovoy}@tudelft.nl

***Abstract*—A novel stepped-amplitude aperiodic phased array synthesis method is proposed. The presented technique is based on iterative convex element position perturbations and uses pre-defined excitation amplitudes. A 64-element irregular array with two discrete amplitude levels (0.5 at the edge-elements and 1 at the center-elements) is synthesized for demonstration purposes. The array achieves a side lobe level lower than -30 dB and a directivity higher than 20 dBi within the given field-of-view ($\pm$60 degrees in azimuth and $\pm$15 degrees in elevation). Through comparative studies of the array directivity, effective isotropic radiated power and maximal side lobe level with the ones of the uniformly-fed/amplitude-tapered periodic arrays and a uniformly-fed aperiodic array, it is shown that the proposed stepped-amplitude array provides the best complexity/performance trade-off.**

***Index Terms*—array synthesis, phased arrays, aperiodic arrays, stepped amplitude arrays.**

I. Introduction

With the introduction of the next generation wireless services, the need and demand for innovative phased array solutions that can achieve better cost/performance trade-offs than the traditional array architectures has increased significantly. The applications are very various, including, but not limited to, communications, radar, sensing and imaging systems.

As discussed in [1], unconventional arrays based on irregular architectures provide a viable solution to relax the complexity challenges. Examples of such configurations include clustered [2], [3], thinned [4], [5], sparse [6], [7] and density-tapered [8], [9] arrays. In clustered arrays, the amplitude weights (in the case of partial clustering), and phase shifts/time delays (in the case of full clustering), are grouped at the sub-array level. In thinned arrays, certain elements on a fixed array grid are switched on/off. In sparse arrays, starting from a very dense fixed topology, the element excitations are computed to satisfy the given radiation pattern criteria with the smallest number of elements. In density-tapered arrays, an irregular layout is synthesized for the given number of elements, based on flexible (gridless) movement of each element.

To realize the above-mentioned architectures with satisfying electromagnetic performance, it is necessary to apply optimization techniques on the amplitude/phase/position of the array elements. Several examples from the literature based on different combinations of amplitude, phase and position optimization is given in Table I. Among all the techniques mentioned, the amplitude-phase-position control yields the highest beamforming flexibility, but at the expense of the largest implementation complexity. Optimizing the amplitudes with no dynamic range control may lead to extremely low power efficiency. Similarly, for nonlinear phase shifts, the array efficiency may decrease significantly. On the other hand, position-only control with uniform excitation amplitudes and linearly progressing phases can provide optimal power efficiency with relatively low side lobe levels (SLLs), which is a crucial factor for effective interference mitigation [16]. The price to pay is the increased integration, fabrication and calibration challenges due to the aperiodic layouts.

Despite shown to be very effective in SLL suppression for large arrays (>256 elements) [17], position-only optimization in a small/medium-sized array will not be able to satisfy the low-sidelobe (<-30 dB) requirements of the next generation high-capacity/connectivity systems [18]. To address this issue to a certain extent, stepped-amplitude arrays with layout irregularity were proposed [15], [19], [20]. As there are only a few discrete amplitude levels, such arrays can maintain a low number of control points and high efficiency [20], can be realized by using only a few amplifier types working at their optimal operating points or can be designed in a partially-clustered arrangement [21], although with additional practical implementation challenges due to the layout irregularity.

In their recent publications [22], [23], the authors proposed an original position-only array synthesis technique based on convex optimization with joint capabilities on uniform-amplitude excitation, minimal element spacing control, multi-beam compatibility, beamwidth reconfigurability, powerful SLL suppression and computational efficiency. The aim of this paper is to extend the study to the stepped-amplitude arrays for

TABLE I
Sample references on combinations of element amplitude, phase and position optimization strategies in array synthesis

Array optimization strategy	Sample reference #
Amplitude-phase-position	[10]
Amplitude-phase	[11]
Amplitude-position	[12]
Position-phase	[13]
Phase-only	[14]
Position-only	[15]

further SLL improvement, and to investigate the performance trade-offs in terms of the array directivity and the effective isotropic radiated power (EIRP).

The rest of the paper is organized as follows. Section II briefly presents the array synthesis strategy by formulating the optimization problem. Section III provides the settings used in the simulations and the corresponding results. Section IV concludes the paper.

II. Array Synthesis Strategy

In this section, a brief summary of the iterative convex element position optimization algorithm introduced in [22] is given, with the addition of non-uniform (in our case, stepped) excitation amplitudes.

Let us assume a pre-given initial layout with a total number of N elements (i.e. $n = 1, 2, ..., N$). Consider that we move the n^{th} element by ϵ_n^i in the $\hat{\mathrm{x}}$ direction (i.e. $x_n^i = x_n^{i-1} + \epsilon_n^i$) and δ_n^i in the $\hat{\mathrm{y}}$ direction (i.e. $y_n^i = y_n^{i-1} + \delta_n^i$) at the i^{th} step of the algorithm. For sufficiently small perturbations on the element locations (i.e. $|(\epsilon, \delta)_n^i| \ll \lambda/2\pi = 0.16\lambda$), the far field function can be linearized around the element positions using the first-order Taylor expansion, which, for linear phase shifts, results in the following approximate relation if the sufficiently small higher order terms $(\epsilon_n^i)^2, (\delta_n^i)^2, (\epsilon_n^i \delta_n^i)$ are removed:

$$f_{\epsilon_n,\delta_n}^{i,s}(u,v) \approx \frac{1}{N}\sum_{n=1}^{N} E_n^i(u,v) e^{jk((u-u_s)x_n^{i-1}+(v-v_s)y_n^{i-1})} w_n(1 + jk(u-u_s)\epsilon_n^i + jk(v-v_s)\delta_n^i) \quad (1)$$

In (1), $f_{\epsilon_n,\delta_n}^{i,s}(u,v)$ represents the normalized far field in $u = \sin\theta\cos\phi, v = \sin\theta\sin\phi$ coordinates at the i^{th} iteration for a scanned beam, s ($s = 1, 2, ..., S$). $E_n^i(u,v)$ represents the embedded element pattern of the n^{th} element at the i^{th} iteration. w_n shows the excitation amplitude of the n^{th} element, which is defined as an input and fixed.

Next, let us define the side lobe region of each scanned beam, $s = 1, ..., S$. Although it changes with scanning, the side lobe regions can be roughly determined using (2) according to the half main lobe width, r, which is about λ/D radians where D is the array's side length.

$$(u,v) \in (\boldsymbol{u},\boldsymbol{v})_{SL,s} \; if \; (u-u_s)^2 + (v-v_s)^2 > r^2 \quad (2)$$

Moreover, the desired minimal element separation, $d_{\min}$ can be defined for every element pair (α, β) using the relation in (3) which is given as a convex approximation to the standard Euclidian distance inequality $(x_\alpha^i - x_\beta^i)^2 + (y_\alpha^i - y_\beta^i)^2 \geq d_{\min}^2$.

$$(\epsilon_\alpha^i - \epsilon_\beta^i)(2x_\alpha^{i-1} - 2x_\beta^{i-1}) + (\delta_\alpha^i - \delta_\beta^i)(2y_\alpha^{i-1} - 2y_\beta^{i-1}) + (x_\alpha^{i-1} - x_\beta^{i-1})^2 + (y_\alpha^{i-1} - y_\beta^{i-1})^2 \geq d_{\min}^2 \quad (3)$$

Thus, the final optimization problem is formulated as

$$\min_{\boldsymbol{\epsilon}^i, \boldsymbol{\delta}^i} \rho, \; s.t. \; \begin{cases} |f_{\boldsymbol{\epsilon}^i,\boldsymbol{\delta}^i}^{i,u_s,v_s}((\boldsymbol{u},\boldsymbol{v})_{SL,s})| \leq \rho \text{ holds } \forall s, \\ |\boldsymbol{\epsilon}^i| \leq \mu, \; |\boldsymbol{\delta}^i| \leq \mu, \; (3) \text{ holds } \forall(\alpha,\beta) \end{cases} \quad (4)$$

where $\boldsymbol{\epsilon}^i = \begin{bmatrix} \epsilon_1^i & \cdots & \epsilon_N^i \end{bmatrix}$ and $\boldsymbol{\delta}^i = \begin{bmatrix} \delta_1^i & \cdots & \delta_N^i \end{bmatrix}$. ρ denotes the maximal SLL which is simultaneously minimized for all the user-defined scan angles. μ is the user-defined upper bound for the position shifts to validate (1).

The optimization problem in (4) is a second order cone programming problem [24], which can be efficiently solved using the Self-Dual-Minimization solver in CVX [25].

III. Simulation Settings and Results

The following common settings are used for the optimization of the aperiodic arrays discussed in this section (Array-C & Array-D, see Fig. 1):

- Number of elements: 64, $d_{\min}$: 0.5λ.
- Embedded element power pattern: $\cos\theta$, $\forall n$.
- $\mu = 0.08\lambda$ (exhibits stable & fast convergence [22]) and $r = 0.28$.
- Field of View (FoV): $\pm 60^o$ / $\pm 15^o$ in azimuth / elevation, as in [18], [21], which is shown with a red rectangle in the pattern contour plots. It is worth to note that in this paper, we aim to minimize the maximal SLL within the FoV. Yet, it is straightforward to modify the algorithm to minimize the SLL over the whole visible space, if that is required by the application.
- $S = 9$, including 1 beam at broadside, 4 beams at the corners of the FoV and 4 beams at the FoV's edge centers, which effectively covers the whole scan range.

The four different array topologies (Array-A, Array-B, Array-C, Array-D) studied in the paper are given in Fig. 1. The value on each element denotes the excitation amplitude. Linearly progressive phases are used for beam steering. A brief description of each topology is given as follows:

- Array-A: First benchmark case, periodic, uniformly-fed, 0.5λ square grid 8x8 array antenna.
- Array-B: Second benchmark case, Array-A with a 30 dB Chebyshev taper.
- Array-C: First optimized array, uniformly-fed, aperiodic. The initial topology for iterative optimization is Array–A.
- Array-D: Second optimized array, stepped-amplitude (with two weight values: 0.5 and 1, as in [15]), aperiodic. The initial topology for optimization is Array–A, but with excitation amplitudes equal to 0.5 at the edge elements (28 elements).

For performance comparison of the four topologies, the directivity patterns for the broadside beam ($u_s = v_s = 0$) and and a beam positioned near the bottom left corner of the FoV ($u_s = -\sin 60^o$, $v_s = -\sin 15^o$) for Array-A, Array-B, Array-C and Array-D are provided in Fig. 2, Fig. 3, Fig. 4 and Fig. 5, respectively. As it may be difficult to extract the relative directivity and SLL information from the $u-v$ plane pattern figures, a sample pattern comparison at the $v = 0$ cut for the broadside beam is given in Fig. 6.

Finally, the performance comparison of the four topologies in terms of the array directivity, EIRP and maximal SLL is given in Table II, both for the broadside beam and the corner beam. In the EIRP calculation, the maximum available power per element, corresponding to excitation amplitude of 1, is taken as 20 dBm.

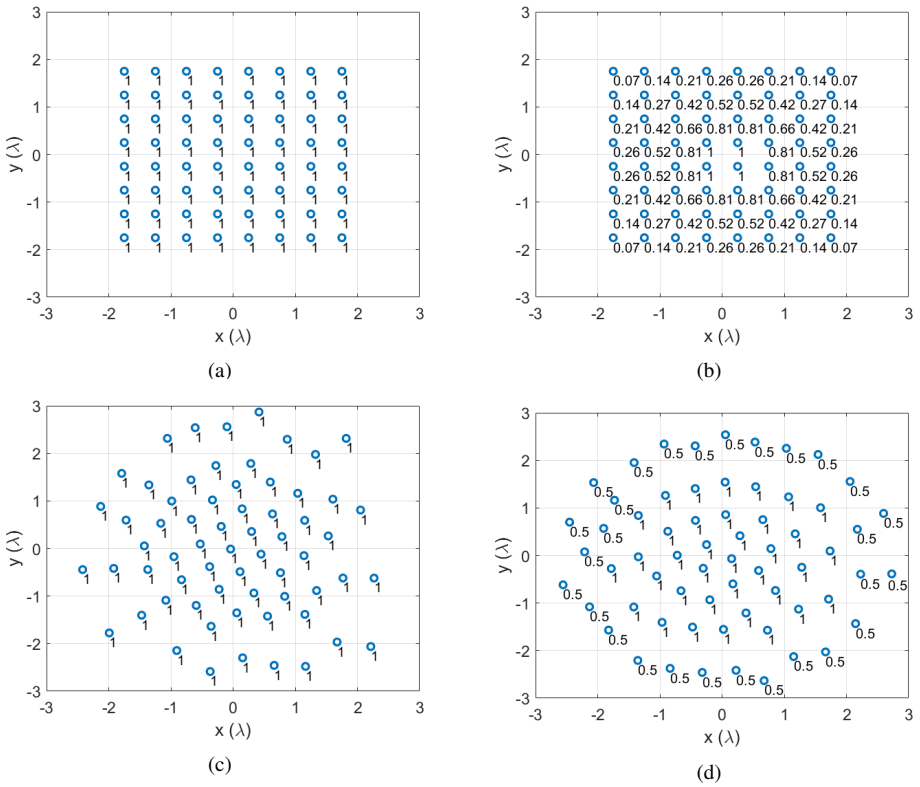

Fig. 1. Array topologies studied in this paper: (a) uniformly-fed periodic array, (b) periodic array with a 30 dB Chebyshev amplitude taper, (c) uniformly-fed aperiodic array, (d) stepped-amplitude aperiodic array.

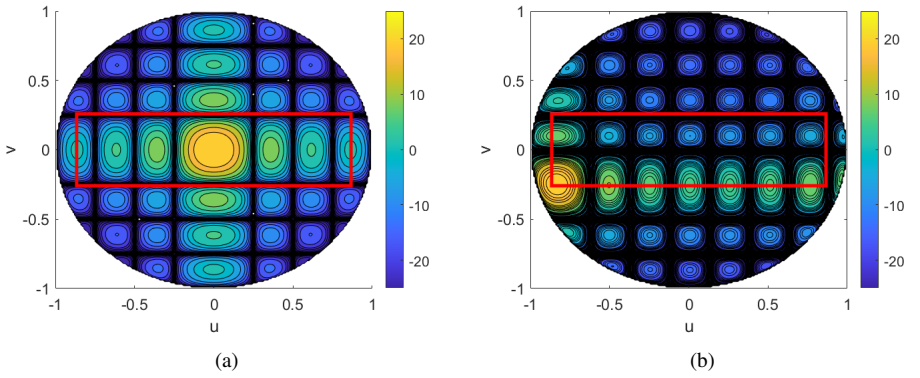

Fig. 2. Directivity (in dBi) pattern of Array-A: (a) broadside beam, (b) corner beam.

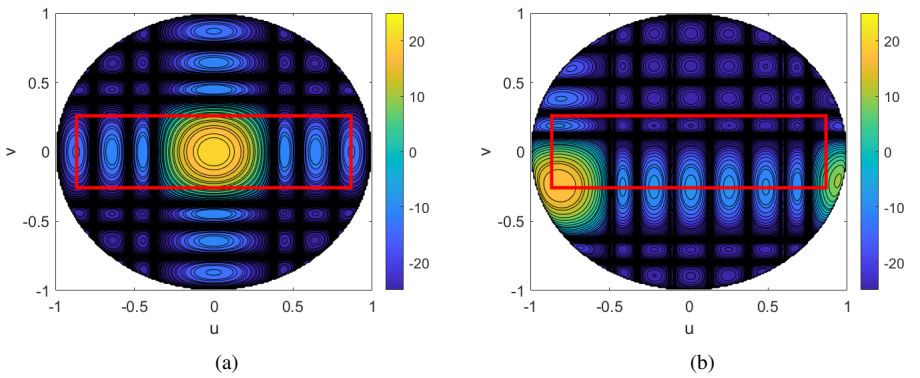

Fig. 3. Directivity (in dBi) pattern of Array-B: (a) broadside beam, (b) corner beam.

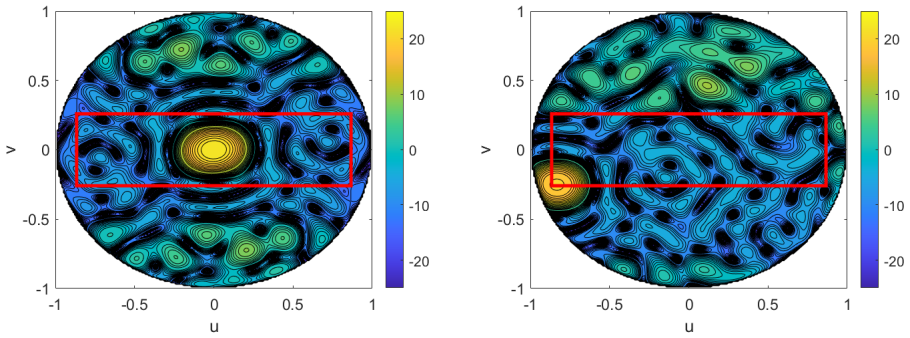

(a) (b)

Fig. 4. Directivity (in dBi) pattern of Array-C: (a) broadside beam, (b) corner beam.

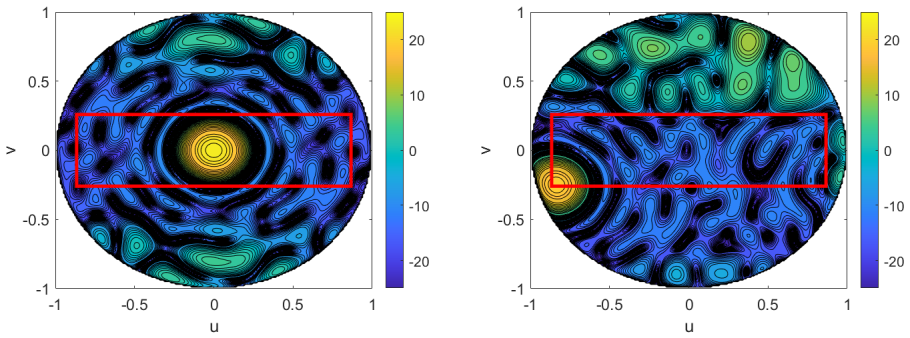

(a) (b)

Fig. 5. Directivity (in dBi) pattern of Array-D: (a) broadside beam, (b) corner beam.

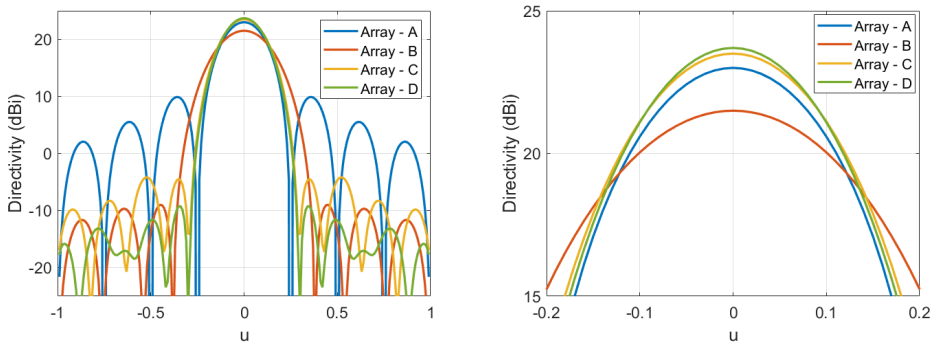

(a) (b)

Fig. 6. Broadside directivity pattern comparison for the four array topologies at the v=0 cut: (a) $|u| \leq 1$, (b) $|u| \leq 0.2$, for beamwidth comparison.

TABLE II
PERFORMANCE COMPARISON OF THE FOUR ARRAY TOPOLOGIES

Array type	Broadside beam			Corner beam		
	Directivity (dBi)	EIRP (dBm)	Maximal SLL (dB)	Directivity (dBi)	EIRP (dBm)	Maximal SLL (dB)
Array-A	23.0	61.1	-13.1	20.4	58.5	-10.4
Array-B	21.5	53.6	-30.5	19.1	51.1	-13.2
Array-C	23.5	61.5	-27.0	20.6	58.7	-23.7
Array-D	23.7	60.0	-32.9	19.9	56.3	-29.6

From the results, the following observations can be made:

- The uniformly-fed periodic array (Array-A) has the simplest architecture, which cannot provide enough SLL suppression capability.
- The amplitude-tapered periodic array (Array-B) can provide low side lobes at broadside, yet its performance gets worse when the beam is scanned towards the edge of coverage. Due to the large dynamic range of amplitudes, the beamwidth gets much larger and the directivity and EIRP is significantly reduced.
- The uniformly-fed aperiodic array (Array-C) provides a high directivity/EIRP (even larger than Array-A due to larger size), while suppressing the SLL to some extent.
- The stepped-amplitude array achieves the lowest SLL ($<$-30 dB) and a similar beamwidth to Array-A and Array-C, while slightly compromising on the EIRP ($\sim$2 dB lower on average as compared to the Array-A and Array-C).

IV. Conclusion

An aperiodic topology synthesis method has been proposed for wide-angle scanning, low-sidelobe stepped-amplitude phased arrays. An iterative convex optimization technique has been used, based on small position perturbations at each element with a user-defined excitation amplitude. A demonstration array with 64 elements and two discrete amplitude levels (0.5 at the edge-elements, 1 at the center-elements) has been synthesized and its directivity, EIRP and SLL performances have been compared with those of the periodic amplitude tapered/non-tapered arrays and an optimized uniformly-fed aperiodic array. It has been pointed out that the stepped-amplitude aperiodic array provides the most favorable radiation pattern characteristics (similar beamwidth and more than 6 dB additional SLL suppression at the expense of around 2 dB reduction in EIRP as compared to the periodic non-tapered/uniformly-fed aperiodic arrays) by achieving the best complexity/performance trade-off.

Interested readers are encouraged to investigate additional study cases with different array sizes, field-of-views, layouts and stepped amplitude distributions as the initial settings of the proposed algorithm.

Acknowledgment

This research was supported in part by Netherlands Organisation for Scientific Research (NWO) and in part by NXP Semiconductors in the framework of the partnership program on Advanced 5G Solutions within the project number 15590 entitled “Antenna Topologies and Front-end Configurations for Multiple Beam Generation”. More information: www.nwo.nl.

References

[1] P. Rocca, G. Oliveri, R. J. Mailloux and A. Massa, “Unconventional phased array architectures and design methodologies—a review,” *Proc. IEEE*, vol. 104, no. 3, pp. 544–560, Mar. 2016.

[2] R. L. Haupt, “Optimized weighting of uniform subarrays of unequal size,” *IEEE Trans. Antennas Propag.*, vol. 55, no. 4, pp. 1207–1210, Apr. 2007.

[3] L. Manica, P. Rocca, and A. Massa, “Design of subarrayed linear and planar array antennas with SLL control based on an excitation matching approach,” *IEEE Trans. Antennas Propag.*, vol. 57, no. 6, pp. 1684–1691, Jun. 2009.

[4] R. L. Haupt, “Thinned arrays using genetic algorithms,” *IEEE Trans. Antennas Propag.*, vol. 42, no. 7, pp. 993–999, Jul. 1994.

[5] D. G. Leeper, “Isophoric arrays - massively thinned phased arrays with well-controlled sidelobes,” *IEEE Trans. Antennas Propag.*, vol. 47, no. 12, pp. 1825–1835, Dec. 1999.

[6] Y. Liu, Z. Nie, and Q. H. Liu, “Reducing the number of antenna elements in a linear antenna array by the matrix pencil method,” *IEEE Trans. Antennas Propag.*, vol. 56, no. 9, pp. 2955–2962, Sep. 2008.

[7] W. Zhang, L. Li, and F. Li, “Reducing the number of elements in linear and planar antenna arrays with sparseness constrained optimization,” *IEEE Trans. Antennas Propag.*, vol. 59, no. 8, pp. 3106–3111, Aug. 2011.

[8] O. M. Bucci, M. D’Urso, T. Isernia, P. Angeletti, and G. Toso, “Deterministic synthesis of uniform amplitude sparse arrays via new density taper techniques,” *IEEE Trans. Antennas Propag.*, vol. 58, no. 6, pp. 1949–1958, Jun. 2010.

[9] M. C. Vigano, G. Toso, G. Caille, C. Mangenot, and I. E. Lager, “Sunflower array antenna with adjustable density taper,” *Int. J. Antennas Propag.*, vol. 2009, 2009.

[10] Y. Liu, Q. H. Liu, and Z. Nie, “Reducing the number of elements in multiple-pattern linear arrays by the extended matrix pencil methods,” *IEEE Trans. Antennas Propag.*, vol. 62, no. 2, pp. 652–660, Feb. 2014.

[11] D. Gies and Y. Rahmat-Samii, “Particle swarm optimization for reconfigurable phase-differentiated array design,” *Microw. Opt. Technol. Lett.*, vol. 38, no. 3, pp. 172–175, Aug. 2003.

[12] G. Prisco and M. D’Urso, “Maximally sparse arrays via sequential convex optimizations,” *IEEE Antennas Wireless Propag. Lett.*, vol. 11, pp. 192–195, Feb. 2012.

[13] D. Jamunaa, G. Mahanti, and F. N. Hasoon, “Synthesis of phase-only position optimized reconfigurable uniformly excited linear antenna arrays with a single null placement,” *J. King Saud Univ. Eng. Sci.*, vol. 32, no. 6, pp. 360–367, Sep. 2020.

[14] Y. Aslan, J. Puskely, A. Roederer, and A. Yarovoy, “Phase-only control of peak sidelobe level and pattern nulls using iterative phase perturbations,” *IEEE Antennas Wireless Propag. Lett.*, vol. 18, no. 10, pp. 2081–2085, Oct. 2019.

[15] B. Fuchs, A. Skrivervik, and J. R. Mosig, “Synthesis of uniform amplitude focused beam arrays,” *IEEE Antennas Wireless Propag. Lett.*, vol. 11, pp. 1178–1181, 2012.

[16] Y. Aslan, J. Puskely, A. Roederer, and A. Yarovoy, “Trade-offs between the quality of service, computational cost and cooling complexity in interference-dominated multi-user SDMA systems,” *IET Comm.*, vol. 14, no. 1, pp. 144–151, Jan. 2020.

[17] Y. Aslan, “Antenna array synthesis and beamforming for 5G applications: an interdisciplinary approach,” Ph.D. dissertation, Dept. Elect. Eng., Math. Comput. Sci., Delft Univ. Technol., Delft, The Netherlands, Aug. 2020.

[18] Y. Aslan, J. Puskely, A. Roederer, and A. Yarovoy, “Effect of element number reduction on inter-user interference and chip temperatures in passively-cooled integrated antenna arrays for 5G,” in *Proc. 14th EuCAP*, Copenhagen, Denmark, Mar. 2020.

[19] M. G. Labate, M. D’Urso, A. Buonanno, and M. Cicolani, “An hybrid strategy for stepped amplitude arrays synthesis,” in *Proc. 2009 EuWiT*, pp. 164–167, Rome, Italy, Sep. 2009.

[20] M. D’Urso, M. G. Labate, and A. Buonanno, “Reducing the Number of Amplitude Controls in Radar Phased Arrays,” *IEEE Trans. Antennas Propag.*, vol. 58, no. 9, pp. 3060–3064, Sept. 2010.

[21] R. Flamini, L. Resteghini, C. Massagrande, C. Mazzucco, F. Morgia, M. Chuan, and R. Lombardi, “Unconventional array for 5G scenario: irregular clustering antenna design and implementation,” in *Proc. 2018 ACES*, Beijing, China, Aug. 2018.

[22] Y. Aslan, J. Puskely, A. Roederer, and A. Yarovoy, “Multiple beam synthesis of passively cooled 5G planar arrays using convex optimization,” *IEEE Trans. Antennas Propag.*, vol. 68, no. 5, pp. 3557–3566, May 2020.

[23] Y. Aslan, A. Roederer, and A. Yarovoy, “Synthesis of optimal 5G array layouts with wide-angle scanning and zooming ability for efficient link setup and high-QoS communication,” *IEEE Antennas Wireless Propag. Lett.*, vol. 19, no. 9, pp. 1481–1485, Sep. 2020.

[24] M. Lobo, L. Vandenberghe, S. Boyd, and H. Lebret, “Applications of second-order cone programming,” *Lin. Algebra Appl.*, vol. 284, no. 1–3, pp. 193–228, 1998.

[25] M. Grant and S. Boyd, “CVX: Matlab software for disciplined convex programming, version 2.1,” Mar. 2014. [Online]. Available: http://cvxr.com/cvx